RSC Advances

PAPER

View Article Online
View Journal | View Issue

Cite this: *RSC Adv.*, 2022, **12**, 20122

Investigation of the anticorrosion and adsorption properties of two polymer compounds on the corrosion of SABIC iron in 1 M HCl solution by practical and computational approaches

M. Abdallah, *[ab] K. A. Soliman,[b] Mubark Alshareef,[a] Arej S. Al-Gorair,*[c] H. Hawsawi,[d] Hatem M. Altass,[a] Salih S. Al-Juaid[e] and M. S. Motawea[bf]

The anticorrosion efficiency of two polymer compounds, namely polystyrene (PS), polybutylene terephthalate (PBT), against the corrosion of SABIC iron (S-Fe) in 1.0 M HCl solution was investigated. The anticorrosion efficiency was estimated by chemical and electrochemical measurements. The anticorrosion efficiency increased with the increase in the concentration of the polymer compounds and reduction in temperature. All the obtained corrosion data confirmed the anticorrosion strength in the presence of PS and PBT compounds, such as the decreasing values of the corrosion current density, capacity of the double layer, and weight reduction, while the values of the charge-transfer resistance increased. Also, the pitting potential values moved in the noble (+) direction. The anticorrosion efficiency of the PBT compound was higher than that of the PS compound, which was 95.98% at 500 ppm concentration for PBT while for PS it was 93.34% according to polarization measurements. The anticorrosion activity occurred by the adsorption of PS and PBT compounds on the surface of S-Fe according to the Langmuir isotherm. The polarization curves indicated that the PS and PBT compounds were mixed-type inhibitors. Density functional theory (DFT) and Monte Carlo simulation (MC) were performed for the two polymer compounds. The computational quantum functions were found to be in agreement with the experimental results.

Received 11th June 2022
Accepted 27th June 2022

DOI: 10.1039/d2ra03614b

rsc.li/rsc-advances

1. Introduction

SABIC iron (S-Fe) is considered one of the most important metals applied in industry, especially in the Kingdom of Saudi Arabia, where it is used in many vital industries, especially in construction.[1,2] HCl solutions are applied for pickling, cleaning, and chemical and electrochemical etching of S-Fe. However, one of the disadvantages of using this acid is that it corrodes S-Fe. In order to diminish the risk of corrosion, scientists have turned to the use of corrosion inhibitors to diminish the rate of corrosion of S-Fe in acidic solution. Generally, organic compounds, especially those containing some hetero atoms in their structure are most commonly utilized as corrosion inhibitors for iron and steels in acidic media.[3–20] The inhibition efficiency of these compounds relies on the concentration of the acidic solution, the nature of the metal or alloy used, the chemical composition of the additives and the capability to adsorb on the metal surface.

There are few studies on the inhibition of S-Fe corrosion in acidic solutions, because its use is concentrated in the Arabian Gulf region. Fawzy *et al.*[21] used synthesized sodium *N*-dodecyl arginine compound as an efficient inhibitor for the corrosion of SABIC iron in acidic, alkaline, and neutral solutions. In previous studies expired antibacterial drugs,[22] expired acyclovir and omeprazole drugs,[23] and expired amoxicillin and cefuroxime drugs[24] have been used as efficacious inhibitors for SABIC iron corrosion in 1.0 M hydrochloric acid solution. The high inhibition efficiency of these expired drugs was due to their strong adsorption on the S-Fe surface. A literature survey revealed that some polymer compounds have been applied to inhibit the corrosion of iron and steels in acidic solutions.[25–32] For instance, polystyrene (PS) and polybutylene terephthalate (PBT) were previously used to inhibit the corrosion of steel in acidic solutions.[33,34] The inhibition effect of these compounds depends on the chemical structure of the polymer and the presence of several active centers that enhance the adsorption process.

This study tested the use of two polymer compounds, namely polystyrene (PS) and polybutylene terephthalate (PBT), to retard

[a]*Chem. Depart., Faculty of Appl. Sci., Umm Al-Qura University, Makkah, Saudi Arabia. E-mail: metwally555@yahoo.com; maabdelsaid@uqu.edu.sa*
[b]*Chem. Depart., Faculty of Sci., Benha University, Benha, Egypt*
[c]*Chem. Depart., College of Sci, Princess Nourah Bint Abdulrahman University, Riyadh, Saudi Arabia*
[d]*University College of Alwajh, Tabuk University, Alwajh, Tabuk, Saudi Arabia*
[e]*Chem. Depart., Faculty of Sci., King Abdulaziz University, Jeddah, Saudi Arabia*
[f]*Chem. Depart., Faculty of Sci., Tabuk University, Tabuk, Saudi Arabia*

the corrosion of S-Fe in 1 M HCl solution. The anticorrosive efficiency of PS and PBT compounds were measured by weight reduction (WR), galvanostatic polarization (GAP), potentiodynamic anodic polarization (PDAP), and electrochemical impedance spectroscopic (EIS) measurements. The thermodynamic functions for the activation and adsorption process were studied. Density functional theory (DFT) approaches were used to predict the corrosion inhibition performance. Theoretical quantum chemical calculations and Monte Carlo simulations were carried out on the studied polymers to correlate with the experimental findings.

2. Experimental

2.1. Materials

All the chemicals used, such as HCl, NaCl, and the tested two polymer compounds, namely PS and PBT, were supplied from Merck or Sigma-Aldrich. Double distilled water was used to prepare the solutions in all the investigations.

2.2. Technologies

SABIC iron (S-Fe) used in various technologies is produced by the Saudi Arabia Basic Industry Company (SABIC) with a purity of 99.99%. For weight reduction (WR), coupons with dimensions of $1 \times 3.8 \times 0.2$ cm^3 were used. The WR of S-Fe in mg was determined after an immersion time of 12 h in free 1 M HCl solutions and as well as in the presence of different concentrations of PS and PBT compounds. For the galvanostatic polarization (GAP), potentiodynamic anodic polarization (PDAP), and electrochemical impedance spectroscopic (EIS), cylindrical or galvanic polarization (GAP), potentiodynamic anodic polarization (PDAP), and electrochemical impedance spectroscopy (EIS) tests, a cylindrical S-Fe rod dipped in Araldites with an uncovered area of 0.38 cm^2 was utilized. Prior to all experiments, the coupons or S-Fe rods were sanded with some grades of sand papers ranging from 300 to 1500 grades, after which they were cleaned with distilled water and acetone and finally dried by filter papers.

WR assays were done as formerly reported.[34,35] GAP and PDAP technologies were performed utilizing a PGSTAT30 potentiostat/galvanostat in a conventional three-electrode cell with a platinum counter electrode (Pt), reference calomel electrode (RCE), and working electrode (S-Fe). In the electrochemical experiments, the electrode was immersed in the test solution until the steady state potential was attained after almost 40 min, and then the polarization started. The potential range for the PDP experiments was −1200 to +200 mV. For the GAP and PDAP tests, the scan rate was adjusted at 2.0 and 0.5 mV s^{-1}, respectively. All the analyses were done at a constant temperature of 303 K in a temperature-controlled system. EIS was done in a frequency range of 100 kHz to 0.1 Hz with an amplitude of 4.0 mV from a peak-to-peak exploitation of AC signals in OCP.

2.3. Anticorrosive compounds

In this study, we used two polymer compounds, namely PS and PBT, as anticorrosive compounds, and these were purchased from Sigma Aldrich. The average molecular weights of PS and PBT were 35 000 and 90 000 g mol^{-1}. The name, chemical structures, and IUPAC names are recorded in Table 1.

2.4. Computational details

In this study, the two polymers were used as corrosion inhibitors for SABIC Fe. To conduct this computational study, the optimized structure geometries of both the dimer and the trimer of butylene terephthalate (D-BT and T-BT) and styrene (D-S and T-S) were found by density functional theory (DFT). The calculations were made using the B3LYP/6-31g(d,p) level of theory in aqueous media using a conductor-like polarizable

Table 1 Chemical structure and IUPAC names of the anticorrosion compounds

IUPAC names	Chemical structure	Name
Poly(1-phenylethene)	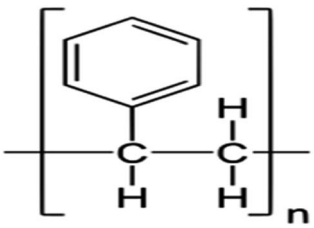	Polystyrene (PS)
Poly(oxy-1,4-butanediyloxycarbonyl-1,4-phenylenecarbonyl)	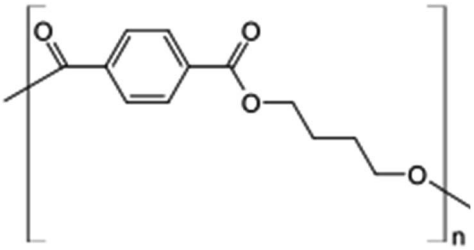	Polybutylene terephthalate (PBT)

continuum (CPCM) model.[36] The energy of the highest occupied molecular orbital (E_{HOMO}), energy of the lowest unoccupied molecular orbital (E_{LUMO}), energy gap (ΔE), global hardness ($\eta = \Delta E/2$), softness ($\sigma = 1/\eta$), back-donation ($\Delta E_{b\text{-}d}$), and dipole moment (μ) were all measured. The calculations were carried out using the Gaussian 09 code.[37]

2.5. Monte Carlo (MC) simulation

We carried out the MC simulation to study the interaction of the dimer polymer with the Fe (110) surface. The goal of this work was to determine the preferential adsorption of the dimer polymer on the iron surface. The simulation protocol was carried out on the Fe (110) plane with a five-layer thickness using the periodic boundary conditions. The Fe (110) plane was magnified to 15 × 15 supercells to provide a large surface area for interaction of the dimer inhibitor with the Fe (110) surface and a 25 Å vacuum was applied over the surface. The condensed-phase optimized molecular potentials for atomistic simulation studies (COMPASS) force field was utilized to search for the equilibrium configuration. The Ewald method was used to illustrate the electrostatic interactions with an accuracy of 1 × 10^{-5} kcal mol^{-1}.[38] The adsorption of the dimer inhibitor over Fe (110) was calculated by the following equation:

$$E_{ads} = E_{Fe+dimer} - E_{dimer} - E_{Fe(110)} \quad (1)$$

where $E_{Fe+dimer}$, E_{dimer}, and $E_{Fe(110)}$ are the energies of the dimer on Fe, energy of the dimer, and energy of the Fe (110), surface respectively.

3. Results and discussion

3.1. GAP tests

GAP curves of S-Fe in 1.0 M HCl solutions alone and in the presence of different concentrations of PS and PBT compounds are presented in Fig. 1A and B, respectively. Some corrosion functions, such as anodic (β_a), cathodic (β_c), and corrosion current density ($I_{corr.}$), which were determined from the intersection of the anodic and cathodic Tafel lines with the corrosion potential ($E_{corr.}$) and anticorrosion efficiency (%AE) were computed and are recorded in Table 2.

The percentage anticorrosion efficiency (%AE_{GAP}) was calculated from the values of $I_{corr.}$ using the following equation:

$$\%AE_{GAP} = \left[1 - \frac{I_{in}}{I_{un}}\right] \quad (2)$$

where I_{in} and I_{un} are the corrosion current densities in the blank 1.0 M Cl solutions and in the presence of different concentrations of the two polymer compounds (PS and PBT) ranging from 100 to 500 ppm.

It is evident that increasing the doses of polymer compounds in 1.0 M HCl solution hindered the anodic dissolution of iron and cathodic H_2 evolution. In the beginning of the GAP curves, there were simultaneous anodic and cathodic curves. After this region, the potential increased with a positive trend (anodic polarization) and decreased with a negative trend (cathodic polarization). From Table 2, we note that the β_a and β_c were nearly constant, whereby the variation in β_a was about 20 mV per decade and the variation in β_c was about 22 mV per decade. These outcomes demonstrate the anticorrosive activity of the two tested polymer compounds occurred through adsorption on the surface of S-Fe according to a blocking adsorption mechanism. The adsorbed PS and PBT reduced the surface area available for anodic iron dissolution and cathodic H_2 evolution reaction without altering the reaction mechanism. The constancy of the Tafel slopes demonstrated that the two polymer compounds (PS and PBT) could be classified as mixed inhibitors. Also, the $E_{corr.}$ values were nearly constant. The variations in the $E_{corr.}$ values were about 15 and 14 mV in the case of the PS and PBT compounds, respectively. These outcomes verified that the PS and PBT compounds were mixed inhibitors. Obviously, the $I_{corr.}$ values decreased significantly, while %AE_{GAP} was elevated at both PS and PBT concentrations. The maximum %AE_{GAP} values were 93.34% and 95.98% at 500 ppm of PS and PBT compounds. It is clear from Table 2 that the %AE_{GAP} for PBT in all the concentrations utilized was more than that of PS. This behavior is explained later in the mechanism of anticorrosive section.

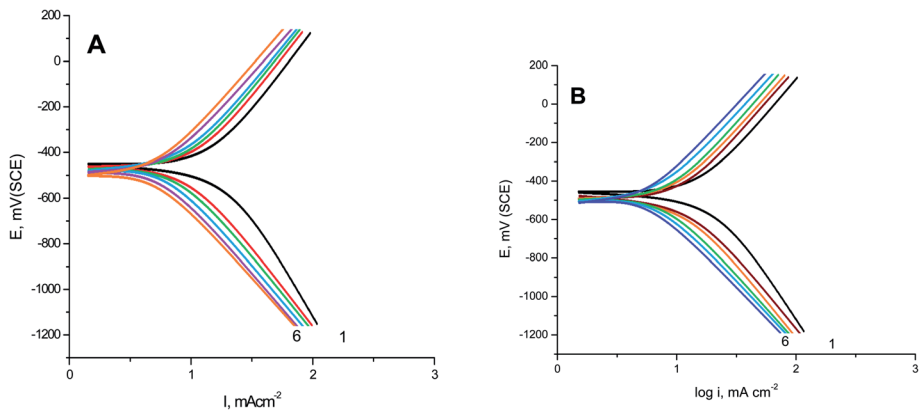

Fig. 1 GAP curves for S-Fe corrosion in the free 1.0 M HCl solution and when containing different concentrations of (A) PS and (B) PBT at 300 K: (1) 0.0, (2) 100, (3) 200, (4) 300, (5) 400, (6) 500 mg l^{-1}.

Table 2 Corrosion parameters obtained from the GAP measurements

Inh.	Inh. conc. (mg l^{-1})	$-E_{corr.}$ mV (SCE)	β_a (mV per decade)	$-\beta_c$ (mV per decade)	$I_{corr.}$ (mA cm^{-2})	$\%AE_{GAP}$
—	0	475	132	180	8.960	—
PS	100	480	135	185	4.122	53.99
	200	482	140	189	2.951	67.06
	300	486	144	192	1.704	80.98
	400	488	148	196	0.851	90.50
	500	490	152	202	0.597	93.34
PBT	100	484	134	184	3.659	59.16
	200	487	142	188	2.329	74.01
	300	492	146	194	1.521	83.02
	400	495	150	200	0.805	91.02
	500	498	154	206	0.449	95.98

3.2. EIS tests

The obtained results from the EIS tests can be stated in terms of the equivalent circuit (Fig. 2), which was applied in the previous embodiment of the SABIC Fe/acid interface.[24] Fig. 3A and B present Nyquist plots for the investigated steel in 1 M HCl with and without different doses of PS and PBT compounds. It is clear from these plots that the semicircle in the presence of PS and PBT is higher than that in the free acid solution which actually providing a protective behavior of the investigated compounds.[39] This behavior is illustrated by the increased values of R_{ct} (Table 3), which could be due to the observed decrease in the C_{dl} values, especially at higher concentrations of additives used. This reveals the adsorption of the additive molecules on the surface of the corrosive CS, instead of the initially adsorbed water molecules.[40] Also, the single semi-circular capacitive ring observed in the free solution indicated a single charge-transfer process controlled the S-Fe corrosion process in this medium.[31] The irregularity of the surface formed at the interface of the S-Fe solution was due to the heterogeneity and coarseness, which led to a decrease in the shape of the semicircle. The $\%AE_{EIS}$ values were computed according to the following equation:

$$\%AE_{(EIS)} = \frac{R_{ct}^{o} - R_{ct}}{R_{ct}^{o}} \quad (3)$$

where R_{ct}^{o} and R_{ct} are the charge-transfer resistance in the blank (1 M HCl) solution and in the presence of PS and PBT compounds, respectively. Whereas the double layer capacitance C_{dl} is given by the following equation:

$$C_{dl} = Y_0(W_{max})^{n-1} \quad (4)$$

where W is the angular frequency, Y_0 and n are, respectively, the values of the CPE admittance and exponent.

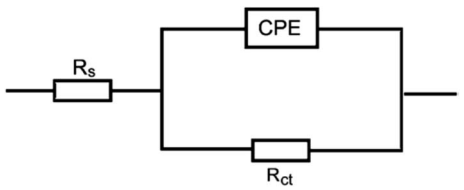

Fig. 2 Electrochemical equivalent circuit applied to fit the EIS measurements.

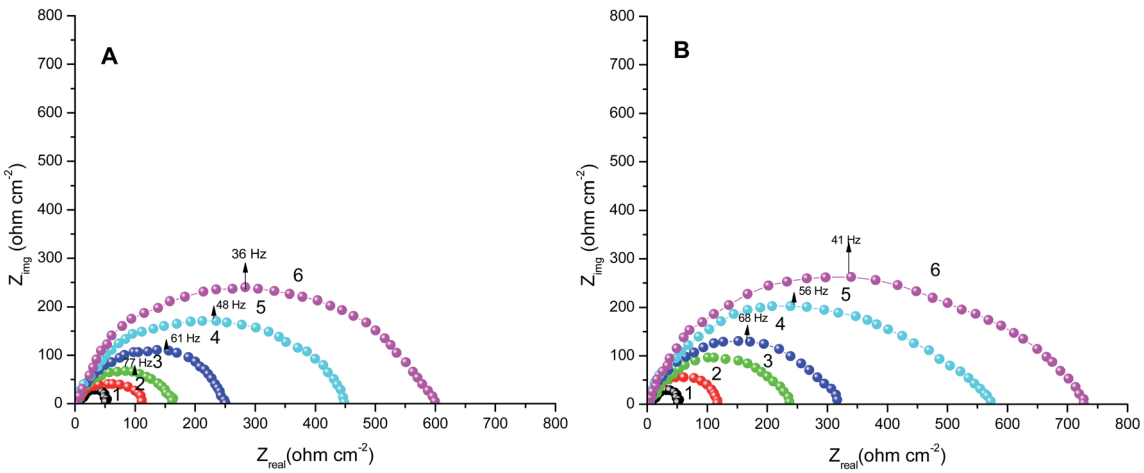

Fig. 3 Nyquist plots for S-Fe corrosion in the blank 1.0 M HCl solution and when containing different concentrations of (A) PS and (B) PBT at 300 K: (1) 0.0, (2) 100, (3) 200, (4) 300, (5) 400, (6) 500 mg l^{-1}.

Table 3 EIS data for S-Fe corrosion in free 1 M HCl solution and with different concentrations of PS and PBT compounds at 300 K

Inh.	Inh. conc. (mg l^{-1})	R_s, ohm cm^{-2}	R_{ct}, ohm cm^{-2}	C_{dl}, (μF cm^{-2})	%AE
—	0	1.2	48	98	—
PS	100	1.3	115	45.4	58.26
	200	1.5	155	38.2	69.03
	300	1.6	245	30.8	80.41
	400	1.9	460	22.4	89.56
	500	2.1	605	17.4	92.07
PBT	100	1.4	120	42.6	60.00
	200	1.6	228	34.4	78.94
	300	1.8	312	28.6	84.61
	400	2.0	570	18.4	91.57
	500	2.2	725	12.6	93.37

$$C_{dl} = \frac{\varepsilon^o \times \varepsilon}{d} S \quad (5)$$

where d is the thickness of the adsorbed film, ε^o is the permittivity of air of the medium, ε is a dielectric constant, and S is the surface area.

The electrochemical parameters, such as R_{ct}, C_{dl}, and $AE_{(EIS)}$%, are recorded in Table 3. It is clear from this table that with the increase in the concentration of PS and PBT compounds, the C_{dl} values decreased due to the gradual replacement of water molecules by the adsorption of polymer compounds on the S-Fe surface, which formed a protective film on the S-Fe surface. For more evidence of the investigated inhibitors action against HCl corrosion, Bode and phase angle plots were made and are presented in Fig. 4A and B. As shown in the plots, the impedance modulus increased with the increase in the additive concentration at low frequencies, hence proving the adsorption of the PS and PBT compounds on the S-Fe surface, thus improving the inhibitory effect against HCl solution.[41] Also, the appearance of a single peak in the phase angle diagrams illustrated the existence of a single time constant at the iron–solution interface.

3.3. PDAP measurements

PS and PBT compounds were examined as pitting corrosion inhibitors by utilizing PDAP measurements. Fig. 5A and B present the PDAP curves for S-Fe in 1.0 M HCl + 0.5 M NaCl solution and in the presence of some concentrations of PS and PBT compounds, respectively, at a scan rate of 0.2 mV s^{-1}. NaCl solution was applied as a pitting corrosion factor. From this figure, it can be seen that there are no peaks in the anodic scan, which clarified the constancy of the passive film created on the iron surface. The current remained constant until a certain potential, when it rose rapidly due to the demolition of the passive film and formation of the pitting attack. This potential is defined as the pitting potential ($E_{pit.}$).[42,43] With increasing the concentrations of PS and PBT, the values of $E_{pit.}$ moved to the noble (+) direction.

Fig. 6 shows the relationship between the $E_{pit.}$ values and the logarithmic of the concentration of the two polymer compounds (PS and PBT). The same behavior was observed in the cases of the two polymers. Broken lines were obtained. At a lower concentricity (100 and 200 mg l^{-1}) of PS and PBT, the shift in the $E_{pit.}$ values to the noble direction were low, but at a concentricity of more than 200 mg l^{-1}, the $E_{pit.}$ values converted quickly to a noble trend according to the following equation:[44,45]

$$E_{pit.} = \gamma + \beta \log C_{polymer} \quad (6)$$

where, γ and β are constants depending on the nature of the metal or alloy and the inhibitor used.

These outcomes confirmed that the presence of PS and PBT compounds increased the resistance to pitting corrosion. These compounds could thus be classified as pitting corrosion inhibitors. At all concentrations examined, the noble shift of $E_{pit.}$ (more resistance to pitting corrosion) for PBT compounds was more than for PS compounds. This completely agrees with the data acquired from the GAP and EIS measurements.

3.4. Weight reduction

3.4.1. Impact of the polymer concentrations. The impact of different concentrations of PS and PBT compounds ranging from 100 to 500 mg l^{-1} on the dissolution of S-Fe in 1.0 M HCl solution was assessed by applying WR methods. The dissolution of S-Fe depended on the area of the coupons utilized and

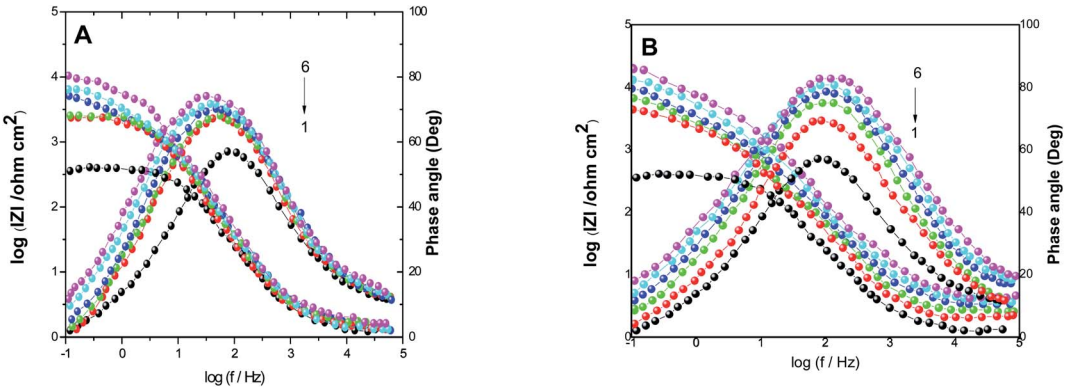

Fig. 4 Bode plots for S-Fe corrosion in the blank 1.0 M HCl solution and when containing different concentrations of (A) PS and (B) PBT at 300 K: (1) 0.0, (2) 100, (3) 200, (4) 300, (5) 400 m (6) 500 mg l^{-1}.

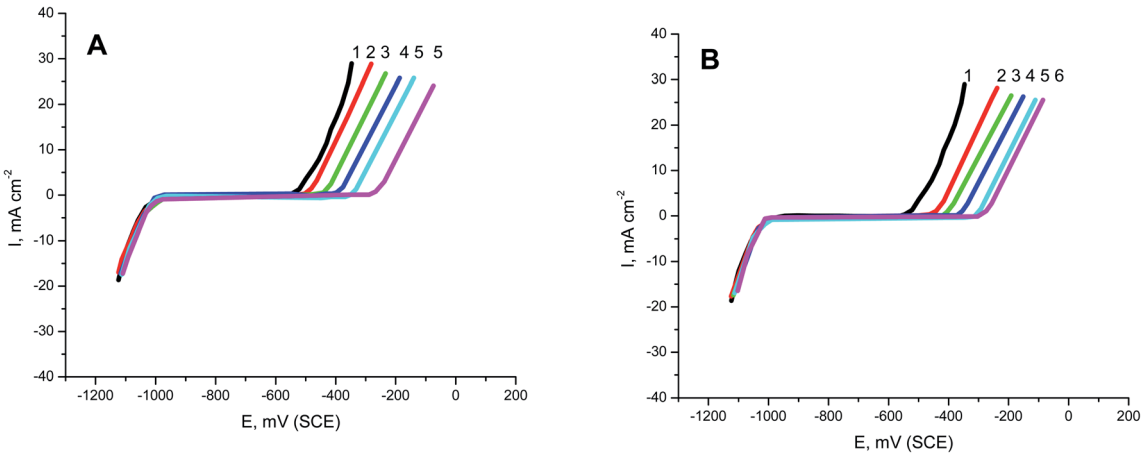

Fig. 5 PDAP curves of S-Fe corrosion in the free 1.0 M HCl + 0.5 M NaCl solution and when containing different concentrations of (A) PS and (B) PBT at 300 K at a scan rate of 0.2 mV s^{-1}: (1) 0.0, (2) 100, (3) 200, (4) 300, (5) 400, (6) 500 mg l^{-1}.

the immersion time. The corrosion rate ($K_{corr.}$) in mg cm^{-1} min^{-1} was computed from the subsequent equation:[43,44]

$$K_{corr.} = \frac{\Delta W}{A \times t} \quad (7)$$

where ΔW in mg equal to $(W_1 - W_2)$ and W_1, W_2 are the weight of S-Fe before and after incubation in the examined solutions, respectively.

The percentage anticorrosion efficiency ($\%AE_{WR}$) and surface coverage (θ) were determined from the values of $K_{corr.}$ using the following equations:[46,47]

$$\%AE_{WR} = \frac{K_{corr.un} - K_{corr.inh}}{K_{corr.un}} \text{ and } \theta = \frac{AE_{WR}}{100} \quad (8)$$

where $K_{corr.un}$ and $K_{corr.inh}$ are the corrosion rates in the blank 1.0 M HCl free solution and in the presence of two polymer compounds (PS and PBT).

The values of WR, $K_{corr.}$, θ, and $\%AE_{WR}$ in the cases of the PS and PBT compounds are listed in Tables 4 and 5, respectively. Cleary from this table, with increasing the concentration of the PS and PBT compounds, the WR decreased, which led to an increase in the $\%AE_{WR}$. These data confirmed the inhibitory power of the two polymer compounds was owing to their strong adsorption on the S-Fe surface. The $\%AE_{WR}$ reached 93.58% and 94.25% in the cases of 500 mg l^{-1} of the PS and PBT compounds, respectively. These data were roughly in agreement with the GAP and EIS results.

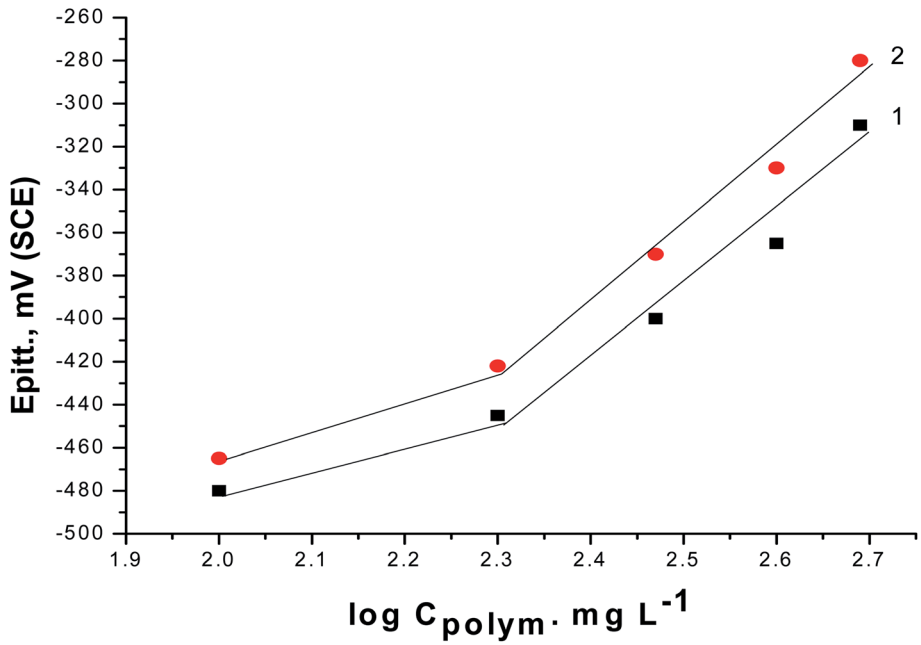

Fig. 6 Relationship between E_{pitt} and the logarithmic concentrations of the two polymer compounds: (1) PS and (2) PBT.

Table 4 Impact of increasing temperature on the corrosion functions acquired from WR measurements for the corrosion of S-Fe in blank 1.0 M HCl and in the presence of different concentrations of PS compounds

Temperature (K)	Conc. of PS (mg l^{-1})	WR (mg)	$K_{corr.} \times 10^{-4}$ mg cm^{-2} h^{-1}	θ	$AE_{(WR)}$%
303	0.00	0.296	10.067	—	—
	100	0.133	4.523	0.551	55.07
	200	0.095	3.231	0.679	67.90
	300	0.059	2.001	0.801	80.12
	400	0.030	1.020	0.899	89.86
	500	0.019	0.646	0.936	93.58
313	0.00	0.389	13.229	—	—
	100	0.191	6.494	0.491	49.09
	200	0.147	4.999	0.622	62.21
	300	0.097	3.298	0.751	75.07
	400	0.058	1.972	0.851	85.09
	500	0.043	1.462	0.889	88.95
323	0.00	0.478	16.256	—	—
	100	0.267	9.081	0.441	44.14
	200	0.205	6.972	0.561	56.11
	300	0.138	4.693	0.711	71.13
	400	0.091	3.095	0.809	80.96
	500	0.076	2.585	0.841	84.09
333	0.00	0.562	19.113	—	—
	100	0.337	11.461	0.400	40.03
	200	0.275	9.355	0.511	51.05
	300	0.185	6.292	0.671	67.08
	400	0.135	4.591	0.760	75.98
	500	0.112	3.809	0.801	80.07

3.4.2. Impact of elevated temperature. The effect of the elevated temperature from 300 K to 330 K on the corrosion data can be seen in the WR measurements of S-Fe in free 1.0 M HCl solution and when including different concentrations of PS and PBT compounds, and the results are tabulated in Tables 4 and 5. As the examined solution temperature increased from 303 K

Table 5 Impact of increasing temperature on the corrosion parameters acquired from WR measurements for the corrosion of S-Fe in blank 1.0 M HCl and in the presence of different concentrations of PBT compounds

Temperature (K)	Conc. of PS (mg l^{-1})	WR (mg)	$K_{corr.} \times 10^{-4}$ mg cm^{-2} h^{-1}	θ	$AE_{(WR)}$%
303	0.00	0.296	10.067	—	—
	100	0.121	4.115	0.591	59.12
	200	0.079	2.687	0.733	73.31
	300	0.053	1.802	0.821	82.09
	400	0.029	0.896	0.919	91.09
	500	0.017	0.578	0.943	94.25
313	0.00	0.389	13.229	—	—
	100	0.167	5.679	0.571	57.07
	200	0.121	4.115	0.689	68.89
	300	0.089	3.026	0.771	77.13
	400	0.054	1.836	0.861	86.12
	500	0.042	1.428	0.892	89.20
323	0.00	0.478	16.256	—	—
	100	0.219	7.448	0.542	54.18
	200	0.192	6.529	0.598	59.83
	300	0.162	5.509	0.661	66.11
	400	0.114	3.877	0.762	76.15
	500	0.100	3.401	0.791	79.08
323	0.00	0.562	19.113	—	—
	100	0.281	9.556	0.500	49.99
	200	0.253	8.604	0.550	54.98
	300	0.213	7.244	0.621	62.10
	400	0.162	5.510	0.712	71.17
	500	0.141	4.795	0.749	74.91

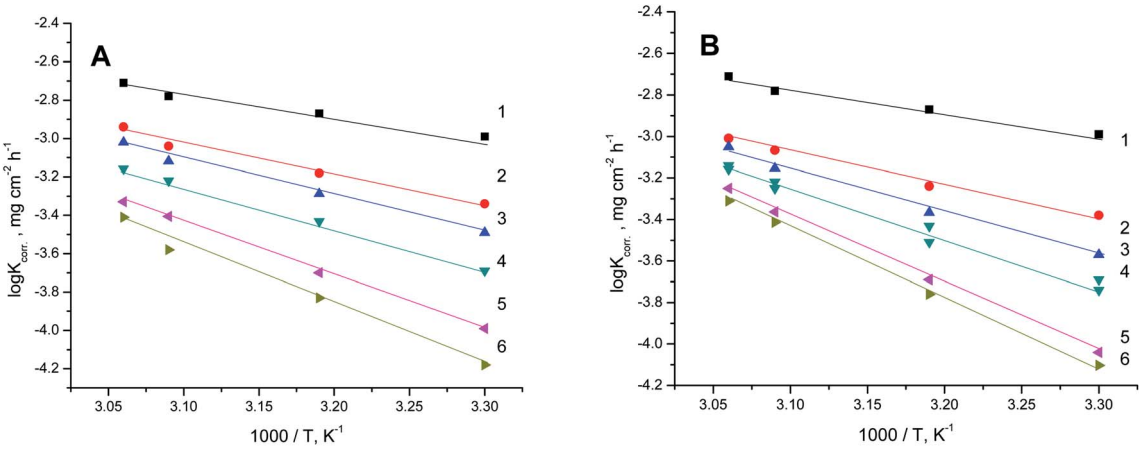

Fig. 7 Plots of log $K_{corr.}$ *versus* 1/*T* for S-Fe in the free 1 M HCl solution and in the presence of different concentrations of (A) PS and (B) PBT compounds. (1) 0.0, (2) 100, (3) 200, (4) 300, (5) 400, (6) 500 mg l^{-1}.

to 333 K, the values of WR and $K_{corr.}$ increased, while the values of θ and $\%AE_{WR}$ declined. This demonstrated the physical adsorption of PS and PBT compounds on the S-Fe surface *via* van der Waals interaction. High temperature may destroy the physical bonds, making the polymer compound desorb from the surface S-Fe.[48–50]

3.4.3. Activation thermodynamic parameters. The values of the activation energy (E_a^*) for the dissolution of S-Fe in the blank 1.0 M HCl solutions and when adding specific concentrations ranging from 100 ppm to 500 ppm of PS and PBT compounds were evaluated by utilizing the Arrhenius equation as follows:[50,51]

$$\log K_{corr.} = \log A - \frac{E_a^*}{2.303RT} \quad (9)$$

where *A*, *R*, and *T* represent the Arrhenius constant, gas constant, and absolute temperature, respectively.

Fig. 7A and B exhibit the plots of log $K_{corr.}$ and 1000/*T* for S-Fe in the 1 M HCl solution alone and in the presence of different concentrations of PS and PBT compounds. Straight lines were obtained with the linear regression coefficients nearly equal to one. The E_a^* values were assessed from the slope of the straight lines and are tabulated in Table 6. Obviously from the this table, it can be seen that the values of E_a^* in the presence of the two polymer compounds were greater than that observed in the blank 1.0 M HCl solution and the values of E_a^* increased with increasing the concentration of PS and PBT compounds. The increased activation energy of S-Fe corrosion indicated that the PS and PBT compounds acted as anticorrosion agents so as to delay the corrosion of S-Fe by the formation of a mass and charge-transfer barrier through them being adsorbed on the surface of S-Fe.

The enthalpy (ΔH^*) and entropy (ΔS^*) of activation were determined by utilizing the following transition state equation:[50,51]

$$\log\left(\frac{K_{corr.}}{T}\right) + \left(\frac{\Delta H^*}{2.303RT}\right) = \left[\left(\log\frac{R}{Nh}\right) + \left(\frac{\Delta S^*}{2.303RT}\right)\right] \quad (10)$$

Table 6 Kinetics parameters for S-Fe in the blank 1 M HCl solution and in the presence of different concentrations of PS and PBT

Conc of inh. (ppm)	E_a kJ mol^{-1}	ΔH^* kJ mol^{-1}	ΔS^* J mol^{-1} K^{-1}
1 M HCl	18.19	14.08	213.51
1 M HCl + 100 ppm PS	22.98	21.16	265.62
1 M HCl + 200 ppm PS	30.72	28.72	303.76
1 M HCl + 300 ppm PS	36.63	32.67	335.42
1 M HCl + 400 ppm PS	40.29	34.46	372.01
1 M HCl + 500 ppm PS	48.86	39.43	398.28
1 M HCl + 100 ppm PBT	26.81	25.68	295.92
1 M HCl + 200 ppm PBT	36.53	30.86	313.86
1 M HCl + 300 ppm PBT	45.95	44.33	356.80
1 M HCl + 400 ppm PBT	58.25	51.44	394.84
1 M HCl + 500 ppm PBT	68.92	60.29	436.26

where *h* and *N* are Planck's constant and Avogadro's number, respectively.

Fig. 8A and B present the relationship between $\log\left(\frac{K_{corr.}}{T}\right)$ *versus* $\left(\frac{1000}{T}\right)$ for S-Fe in the blank 1 M HCl solution and in the presence of different concentrations of PS and PBT compounds. Straight lines were obtained. The ΔH^* and ΔS^* values were computed from the slopes and the intersections of the straight lines and are recorded in Table 6. It is evident from this table that the ΔH^* values were positive in 1 M HCl solution alone and in the presence of different concentrations of the two polymer compounds (PS and PBT). This indicated the endothermic nature of the formation of the activated complexes during the corrosion process. Also, the values of ΔH^* became more positive with increasing the concentrations of the PS and PBT, which made it more difficult for iron to corrode.[52] The values of ΔS^o were negative and became less positive when the concentration of the two polymer compounds increased. This suggested that the compound activated in the rate-limiting step was involved

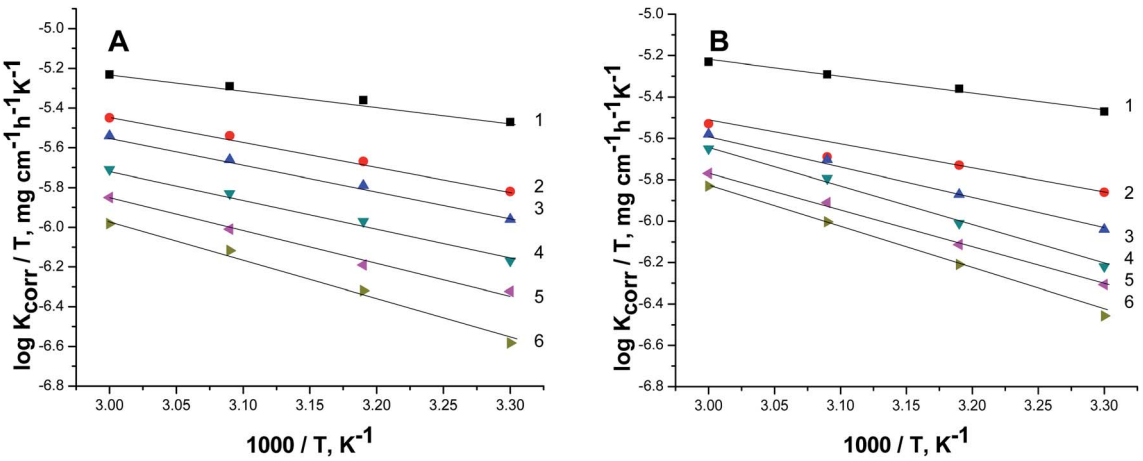

Fig. 8 Plots of log $K_{corr.}/T$ *versus* $1/T$ for S-Fe in the free 1 M HCl solution and in the presence of different concentrations of (A) PS and (B) PBT compounds: (1) 0.0, (2) 100, (3) 200, (4) 300, (5) 400, (6) 500 mg l^{-1}.

in binding not disengagement. This clarifies that the activated molecules were in a less chaotic state than those in the initial stage.[53] The anticorrosion efficiency of PS and PBT compounds with respect to the rise in the values of $E_a^*$and $\Delta H^*$and the decline in the values of ΔS^* followed the order: PBT > PS.

3.5. Adsorption and mechanism of the anticorrosion process

The anticorrosiveness of the two investigated polymer compounds (PS and PBT) on the corrosion of S-Fe in 1 M HCl solution principally relied on its adsorption at the S-Fe surface interface. On the whole, the adsorption operation involves an exchange process between the polymer compounds in the aqueous phase [polymer$_{(aq.)}$] and the number of water molecules adsorbed on the S-Fe surface due to this equation:

$$\text{Polymer}_{(aq.)} + \alpha H_2O_{(surf.)} = \text{polymer}_{(surf.)} + \alpha H_2O_{(aq.)} \quad (11)$$

where α is the amount of adsorbed water molecules that are replaced by one polymer molecule. The adsorption of PS and PBT on the S-Fe surface depended on several factors, including the concentration of the mineral acid and the polymer compounds used, the molar mass of the polymer, the temperature, the presence of certain active centers in the chemical structure of the polymer. The adsorption of the two polymer compounds on the surface of S-Fe diminished the rate of corrosion and elevated the anticorrosion effectiveness. To choose a suitable isotherm for this adsorption, the surface coverage values (θ) were applied to several isotherms. The results obtained confirmed that the preferable isotherm was the Langmuir isotherm, which can be given by:[54]

$$C_{polymer} + \frac{1}{K_{ads}} = \frac{C_{polymer}}{\theta} \quad (12)$$

where $C_{polymer}$ is the concentricity of the polymer used and K_{ads} is the equilibrium constant of adsorption.

Fig. 9A and B present the Langmuir plots ($C_{polymer}$ and $C_{polymer}/\theta$) for the adsorption of the two polymer compounds (PS and PBT) on the surface of S-Fe at altered temperatures ranging from 303 K to 333 K. A straight line with a slope of about one

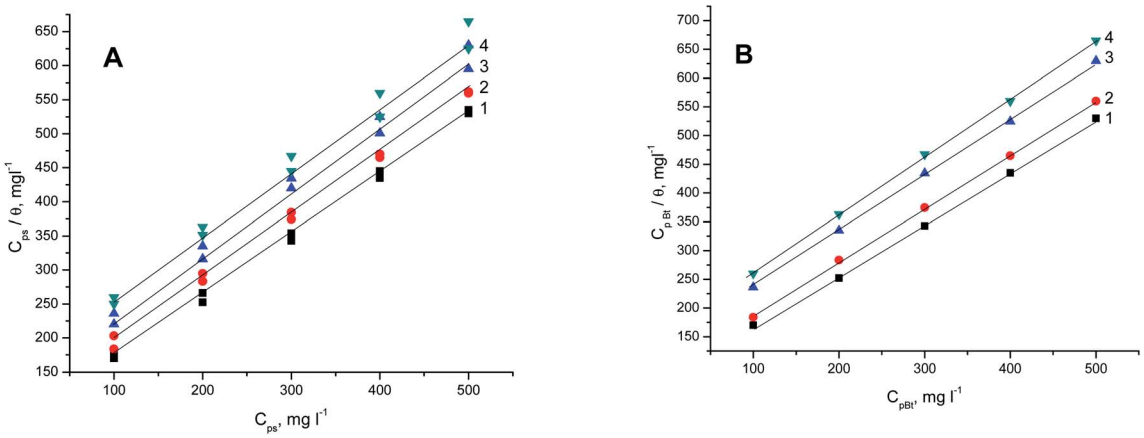

Fig. 9 Langmuir adsorption isotherms for S-Fe in the blank 1 M HCl solution and in the presence of different concentrations of (A) PS and (B) PBT compounds at: (1) 303 K, (2) 313 K, (3) 323 K, (4) 333 K.

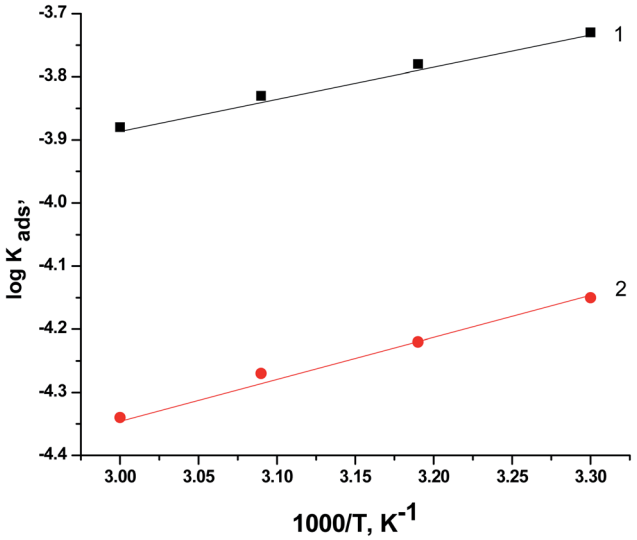

Fig. 10 Plots of log K_{ads} *versus* 1000/T for the corrosion of S-Fe in 1.0 M HCl solution in the presence of PS and PBT compounds at different temperatures: (1) PBT and (2) PS.

was obtained, which confirmed that the Langmuir isotherm was a suitable isotherm. This isotherm assumed there was zero interaction between the adsorbed species on the S-Fe surface. From the intercept of the Langmuir plots, we computed the values of K_{ads}. Specifically, the values of K_{ads} for the PS compounds were computed from Fig. 9A and were (6.45, 5.71, 5.12, and 4.54) $\times 10^{-3}$ mol l^{-1} at temperatures of 303, 313, 323, and 333 K, respectively; while the values of K_{ads} for the PBT compounds were computed from Fig. 9B and were (6.25, 5.40, 4.82, and 4.04) $\times 10^{-3}$ mol l^{-1} at the temperatures of 303, 313, 323, and 333 K, respectively. The values of K_{ads} indicated that both PS and PBT on the surface of S-Fe were readily and cohesively adsorbed on the surface of S-Fe.

The values of free energy of adsorption (ΔG^{o}_{ads}) were determined from the values of K_{ads} according to the following equation:

$$55.5K_{ads} = \exp(-\Delta G^{o}_{ads}/RT) \quad (13)$$

The determined values of ΔG^{o}_{ads} in the presence of PS compounds were −28.32, −27.14, −26.97, and −26.02 kJ mol^{-1} at temperatures of 303, 313, 323, and 333 K, respectively; while the values of ΔG^{o}_{ads} in the presence of PBT compounds were −25.08, −24.42, −24.06, and −23.83 kJ mol^{-1} at temperatures of 303, 313, 323, and 333 K, respectively. It is evident that all the values of ΔG^{o}_{ads} were negative, demonstrating that the adsorption of PS and PBT compounds on S-Fe was spontaneous. Vant's Hoff equation was applied to determine the enthalpy of adsorption ΔH^{o}_{ads} according to the following equation:[55]

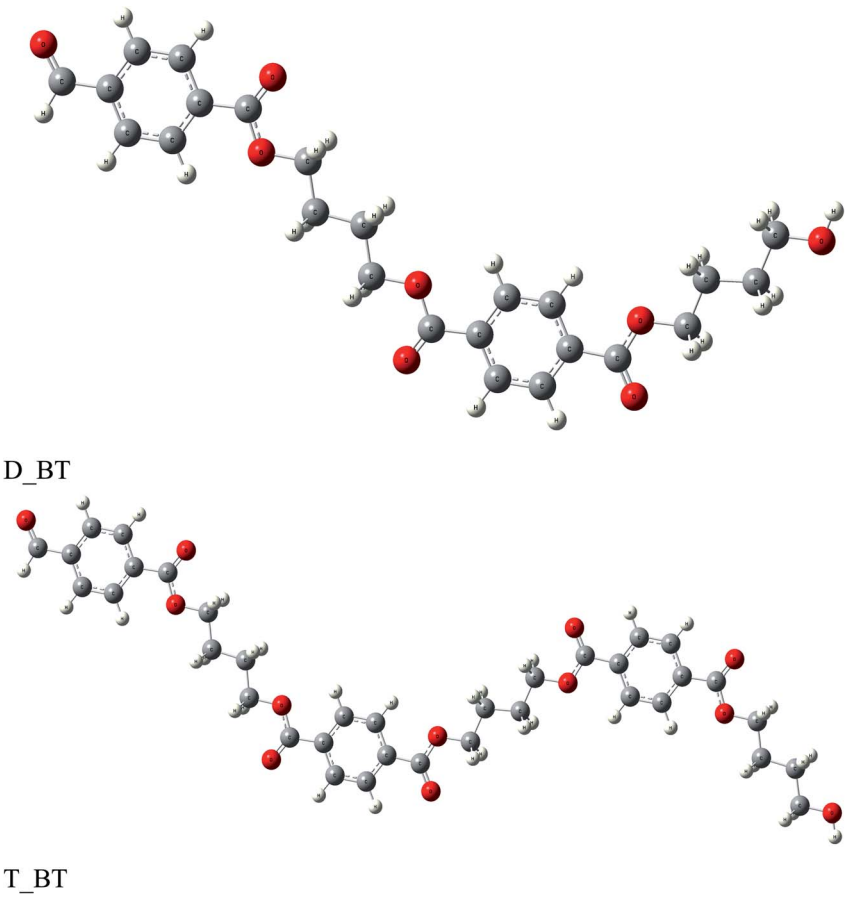

Fig. 11 Optimized structure of di- and tri-butylene terephthalate.

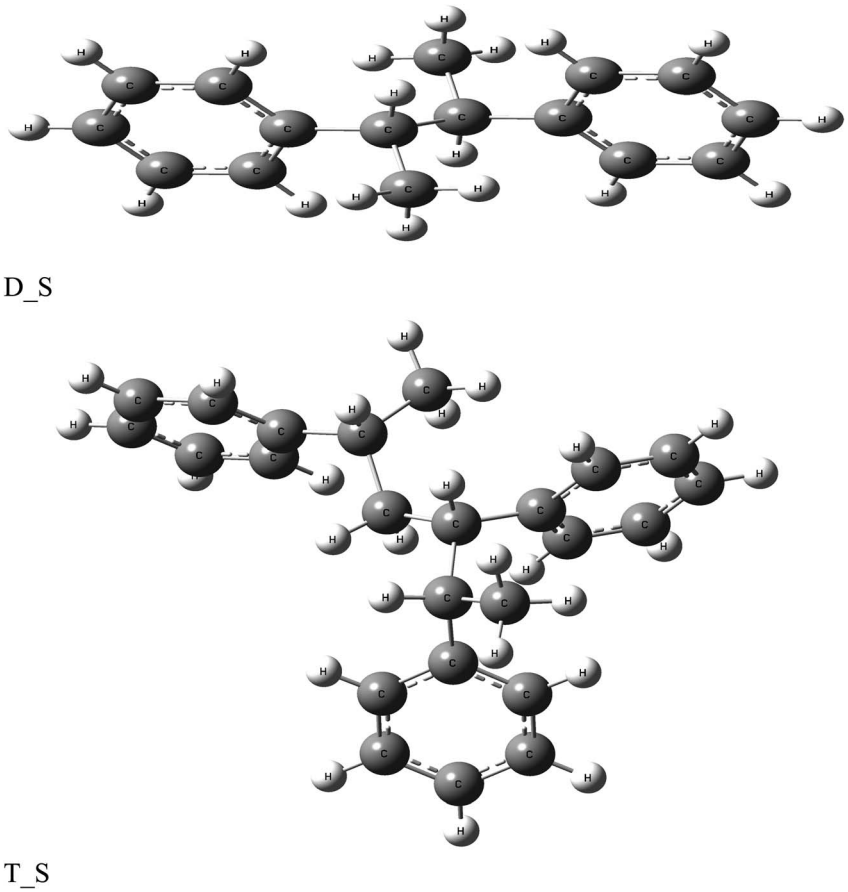

Fig. 12 Optimized structure of di- and tri-styrene.

$$\log K_{ads} = \frac{-\Delta H^{o}_{ads}}{2.303RT} + X \quad (14)$$

where X is a constant.

Fig. 10 displays the relationship between $\log K_{ads}$ *vs.* $1/T$ (Van't Hoff plots) for PS and PBT adsorbed on the surface of S-Fe in 1.0 M HCl solution. Straight lines were obtained. From the slope of the straight lines, we could compute ΔH^{o}_{ads}. The values of ΔH^{o}_{ads} were −19.88 and −21.12 kJ mol^{-1} for PS and PBT compounds, respectively. The negative mark of ΔH^{o}_{ads} indicated that the adsorption of PS and PBT compounds on the S-Fe surface was exothermic.

The entropy of adsorption (ΔS_{ads}) values were obtained from the following equation:

$$\Delta S_{ads} = \frac{\Delta G_{ads} - \Delta H_{ads}}{T} \quad (15)$$

The computed values of ΔS_{ads} for PS compounds were −0.159, −0.086, −0.022, and −0.018 kJ mol^{-1} at temperatures of 303, 313, 323, and 333 K, respectively; while the values of ΔS_{ads} for PBT compounds were −0.013, −0.011, −0.009, and −0.008 kJ mol^{-1} at temperatures of 303, 313, 323, and 333 K, respectively.

The negative markings of ΔS_{ads} indicated that the chaos diminished upon transition from the reactant to the adsorbent surface. This demonstrates the adsorption intensity of the PS and PBT compounds on the surface of S-Fe. The values of the adsorption thermodynamic functions were consistent with the low values of the anticorrosion efficiency at elevated temperatures.

The corrosion functions and the anticorrosion efficiency gained from the various technologies confirmed that the %AE of PS compounds was greater than that of PBT compounds.

Table 7 Quantum parameters for di-, tri- PBT and PS calculated using B3LYP/6-31g(d,p) in the aqueous phase

	E_{HOMO} (eV)	E_{LUMO} (eV)	ΔE (eV)	μ (debye)	σ (eV)$^{-1}$	η (eV)	$\Delta E_{d\text{-}b}$ (eV)
D_PS	−6.39	−0.17	6.22	0.0001	0.32	3.11	−0.78
T_PS	−6.39	−0.19	6.20	0.57	0.33	3.10	−0.77
D_PBT	−7.27	−2.35	4.92	2.41	0.41	2.46	−0.62
T_PBT	−7.27	−2.35	4.92	6.46	0.41	2.46	−0.62

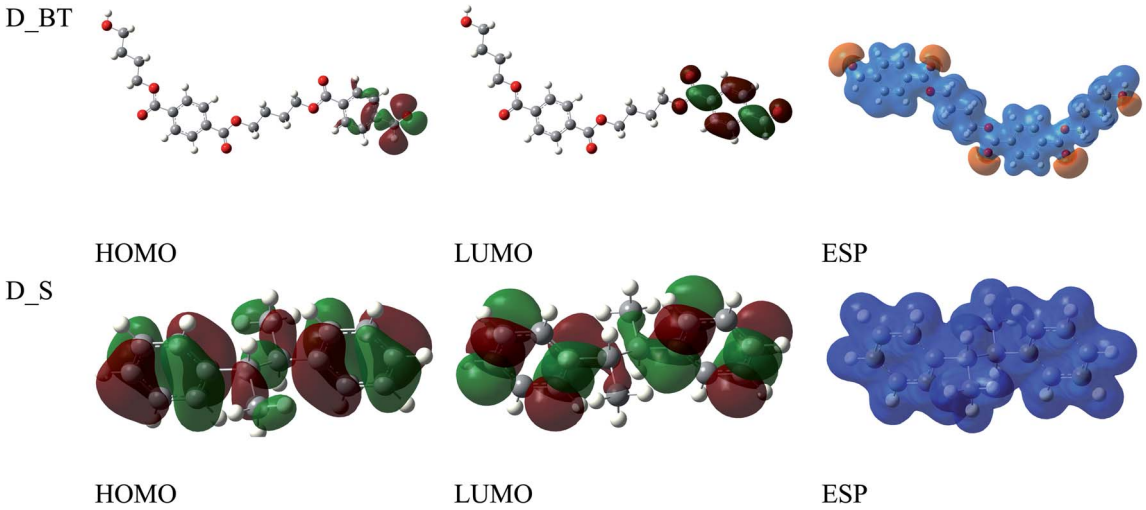

Fig. 13 Frontier orbitals and ESP of di-butylene terephthalate and di-styrene.

These outcomes can be explicated on the basis of the molar mass of the polymer compound tested, where the molar mass of PBT is greater than that of PS. Thus PBT compounds will create a larger protective-layer covering on the surface than PS, giving a higher anticorrosion efficiency. This layer isolates the surface of the iron from the corrosive acidic solution and prevents contact of the S-Fe surface with the acidic solution.

The results of the PDAP measurements showed that the PS and PBT compounds had a high ability to resist the pitting corrosion by shifting the value of the pitting potential to the noble (+) direction. The resistance of pitting attack can be explicated by the competitive adsorption that occurred on the S-Fe surface between Cl^- ions and the PS and PBT compounds to reach the surface of S-Fe until the polymer compounds became dominant. This led to the formation of a protective layer on the surface of S-Fe, which impeded the pitting attack of chloride ions.

3.6. Computational study

The anticorrosion efficiency of the dimer and trimer of butylene terephthalate and styrene were investigated by finding the quantum parameters that correlated with the practical outcomes. The optimized geometries of the dimer and trimer of the two inhibitors are presented in Fig. 11 and 12. The optimizations were obtained by using the B3LYP level of theory. As shown in Table 7, most the quantum parameter values for the dimer and trimer of the butylene terephthalate inhibitor were the same, but there were slight changes between the dimer and trimer of the styrene inhibitor, so the frontier orbitals, molecular electrostatic potential, and adsorption of the polymer on the iron surface were investigated using the dimer molecules. The frontier molecular orbital (HOMO and LUMO) distributions could show the active sites that the inhibitors possess to interact with a metallic surface. As seen in Fig. 13, for the dimer of butylene terephthalate the HOMO was concentrated on the benzaldehyde moiety and LUMO in the terephthalate region, while the HOMO and LUMO distributions of the dimer of styrene were the same, indicating a high chance of electron transfer from the HOMO to the LUMO with bonding formation between the tested reagents.[54] The high values of E_{HOMO} are likely to indicate a molecule's tendency to donate electrons to suitable acceptor molecules with empty molecular orbitals. The LUMO energy reflects a molecule's ability to receive electrons. So, with increasing the HOMO and lowering the LUMO energy levels, the inhibitor's ability to attach to the metal surface is improved. As shown in Table 7, the E_{HOMO} and E_{LUMO} of the dimer of butylene terephthalate were lower than the dimer of styrene. The energy gap (ΔE) is another parameter that is correlated with the anticorrosion efficiency. A lower energy gap value indicates a higher inhibition efficiency, because the energy of removing an electron from the highest occupied orbital is low;[55] therefore, the higher reactivity of an inhibitor toward adsorption on metallic surfaces. The results obtained, as seen in Table 7, indicate that the dimer of butylene terephthalate had better anticorrosion efficiency than the dimer of styrene.

The dipole moment (μ) is an index for predicting the direction of a corrosion inhibition process. The dipole moment is a measurement of polarity in a bond, which is linked to the electron distribution in a molecule. It is generally accepted that the adsorption of polar compounds with high dipole moments on the metal surface should result in improved anticorrosion efficiency. As shown in Table 7, the dipole moment of the dimer of butylene terephthalate was higher than that of the dimer of the styrene inhibitor, which showed a high symmetry of 0.0001 debye; therefore, the dimer of butylene terephthalate had a better anticorrosion efficiency than the dimer of styrene, which agreed with the experimental results.

The molecular electrostatic potential (ESP) is an important quantitative descriptor used to determine the reactive sites of electrophilic and nucleophilic attacks. As seen in Fig. 13, the negative electrostatic potential (red regions) for the dimer of butylene terephthalate was concentrated on the oxygen atom of C=O, indicating the acceptor sites. The positive electrostatic

potential (blue regions) for the dimer of styrene was concentrated in all the molecules, which were thus associated with donor sites.

The softness (σ) and hardness (η) are called global reactivity descriptors. These parameters can be used to obtain the reactivity and stability of a molecule. The adsorption of polymer molecules on the S-Fe surface occur with a molecule that has a higher value of softness. Global hardness is a measure of the molecular resistance to electron cloud polarization or deformation due to minor chemical reaction disturbances. Soft molecules have a small energy gap but hard molecules have a higher energy gap.[56] Generally, the inhibitor with the highest value of softness gives the highest anticorrosion efficiency.[57,58] As presented in Table 7, the dimer of butylene terephthalate with a softness of 0.41 had the highest anticorrosion efficiency.

The back-donation of electrons ($\Delta E_{b\text{-}d}$) increases with the increase in anticorrosion efficiency. As shown in Table 7, this suggests the dimer of butylene terephthalate enhanced the back-donation when compared with the dimer of styrene.

3.7. MC simulation

The interaction assessment of the two dimers of butylene terephthalate and styrene on the Fe (110) surface was performed using Monte Carlo simulation.[59] Fig. 14 shows the most stable adsorption configurations of the polymer molecule on the Fe (110) surface. The dimer of butylene terephthalate was adsorbed in parallel on the Fe (110), but for the dimer of styrene, we found that the molecule was adsorbed by the two benzene rings tilted on the Fe (110) surface. When comparing the adsorption energy of the two inhibitors, as presented in Table 8, the dimer of butylene terephthalate had a higher adsorption energy than the dimer of styrene. These results confirmed the dimer of butylene terephthalate had a higher anticorrosion efficiency

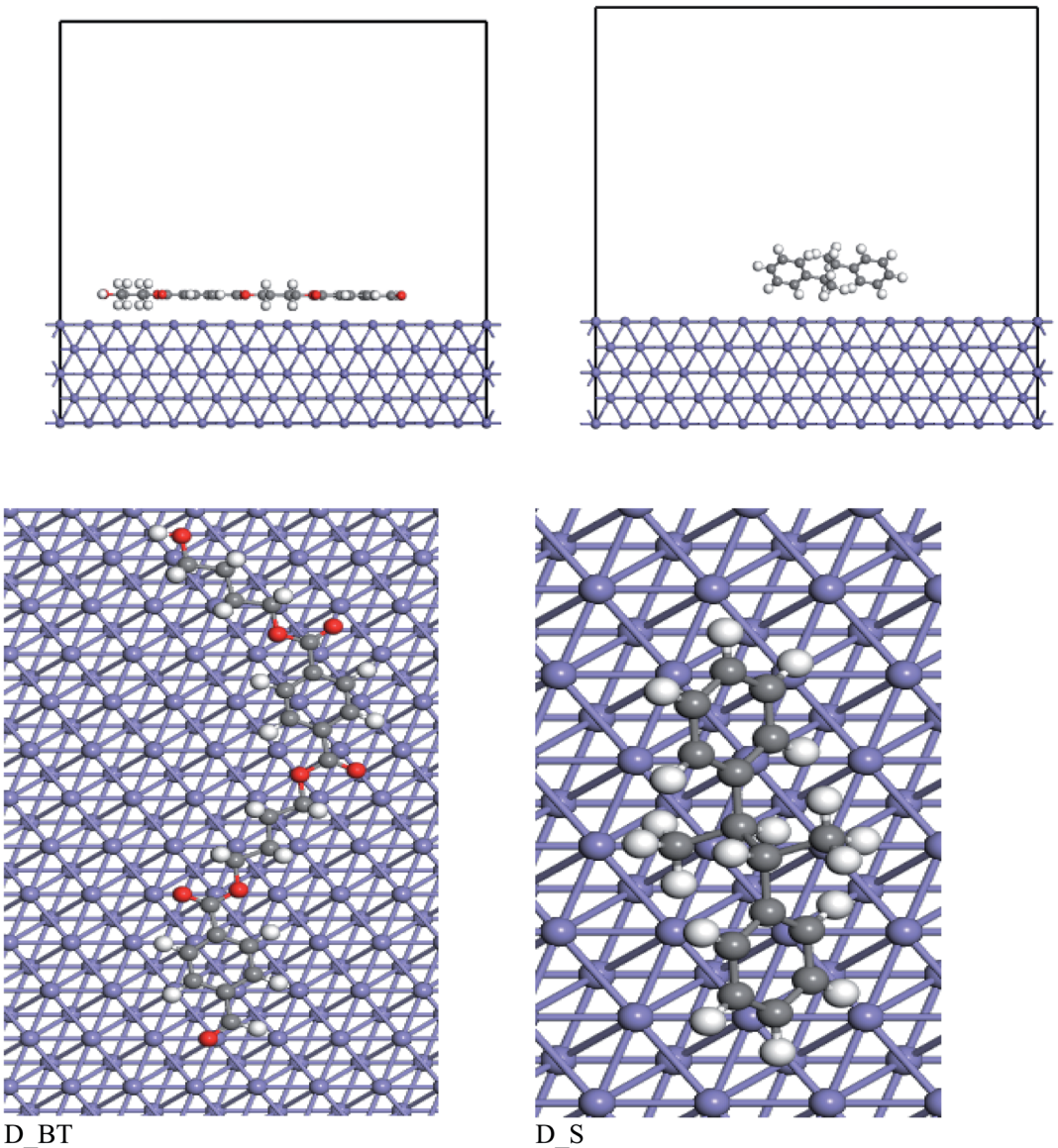

Fig. 14 Top and side views for adsorption of the two dimers over Fe (110) surface.

Table 8 Adsorption energies of the two dimer inhibitors over the Fe (110) surface

System	Adsorption energy (kcal mol^{-1})
D_PS + Fe (110)	−82.95
D_PBT + Fe (110)	−231.06

than the dimer of styrene. These results coincided with the experimental anticorrosion efficiencies.

4. Conclusions

The two polymer compounds (PS and PBT) acted as a good inhibitor for the corrosion of S-Fe in 1.0 M HCl solution. The anticorrosive efficiency rises with rising the concentrations of PS and PBT compounds. All the chemical, electrochemical and theoretical studies confirm that the anticorrosive efficiency of PBT is more than PS compound. The anticorrosive strength of these compounds was explicated by vigor spontaneous adsorption of these compounds on the S-Fe surface. The adsorption obeyed Langmuir isotherm. This theoretical study aims to compare the two polymer inhibitors based on quantum descriptors obtained by DFT. MC simulation was employed to determine the picture of the inhibitor molecule over the Fe (110) surface. The theoretical parameters are in agreement with experimental results.

Conflicts of interest

There are no conflicts to declare.

Acknowledgements

The authors would like to thank the Deanship of Scientific Research at Umm Al-Qura University for supporting this work with a grant, Grant Code: (22UQU4320006DSR01)

References

1 M. Abdallah, A. S. Al-Gorair, A. Fawzy, H. Hawsawi and R. S. Abdel Hameed, Enhancement of adsorption and anticorrosion performance of two polymeric compounds for the corrosion of SABIC carbon steel in hydrochloric acid, *J. Adhes. Sci. Technol.*, 2022, **36**, 35–53.

2 M. Abdallah, A. Fawzy, H. Hawsawi, R. S. A. Hameed and S. S. Al-Juaid, Estimation of Water-Soluble Polymers (Poloxamer and Pectin) as Corrosion Inhibitors for Carbon Steel in Acidic Medium, *Int. J. Electrochem. Sci.*, 2020, **15**, 8129–8144.

3 Z. Hajiahmadi and Z. Tavangar, Extensive theoretical study of corrosion inhibition efficiency of some pyrimidine derivatives on iron and the proposal of new inhibitor, *J. Mol. Liq.*, 2019, **284**, 225–231.

4 R. S. Abdel Hameed, A. H. Al-Bagawi, H. A. Shehata, A. H. Shamroukh and M. Abdallah, Corrosion Inhibition and Adsorption Properties of Some Heterocyclic Derivatives on C-Steel Surface in HCl, *Journal of Bio- and Tribo-Corrosion*, 2020, **51**(6), 1–11.

5 R. S. Abdel Hameed and M. Abdallah, Corrosion inhibition of carbon steel in 1.0 M hydrochloric acid using some pyrazolo[3,4-d]Pyrimidnone derivatives, *Prot. Met. Phys. Chem. Surf.*, 2018, **54**, 113–121.

6 M. Abdallah, H. M. Altass, B. A. AL Jahdaly and M. M. Salem, Some natural aqueous extracts of plants as green inhibitor for dissolution of carbon steel in 0.5 M sulfuric acid, *Green Chem. Lett. Rev.*, 2018, **11**, 189–196.

7 M. Abdallah, E. A. Helal and A. S. Fouda, Amino pyrimidine derivatives as inhibitors for corrosion of 1018 carbon steel in nitric acid solutions, *Corros. Sci.*, 2006, **48**, 1639–1654.

8 X. Li, S. Deng and H. Fu, Allyl thiourea as a corrosion inhibitor for cold rolled steel in H_3PO_4 solution, *Corros. Sci.*, 2012, **55**, 280–288.

9 J. H. Al-Fahemia, M. Abdallah, E. A. M. Gad and B. A. AL Jahdaly, Experimental and theoretical approach studies for melatonin drug as safely corrosion inhibitors for carbon steel using DFT, *J. Mol. Liq.*, 2016, **222**, 1157–1163.

10 F. Benhiba, R. Hsissou, Z. Benzekri, M. E. Belghiti, A. Lamhamdi, A. Bellaouchou, A. Guenbour, S. Boukhris, H. Oudda, I. Warad and A. Zarrouk, Nitro substituent effect on the electronic behavior and inhibitory performance of two quinoxaline derivatives in relation to the corrosion of mild steel in 1 M HCl, *J. Mol. Liq.*, 2020, **312**, 113367.

11 M. Abdallah, H. M. Altass, A. S. Al-Gorair, J. H. Al-Fahemi and K. A. Soliman, Natural nutmeg oil as a green corrosion inhibitor for carbon steel in 1.0 M HCl solution: Chemical, electrochemical and computational methods, *J. Mol. Liq.*, 2021, **323**, 115036.

12 M. Abdallah, N. El Guesmi, A. S. Al-Gorair, R. El-Sayed, A. Meshabi and M. Sobhi, Enhancing the anticorrosion performance of mild steel in sulfuric acid using synthetic non-ionic surfactants: Practical and Theoretical Studies, *Green Chem. Lett. Rev.*, 2021, **14**(2), 382–394.

13 A. Berrissoul, E. Loukili, N. Mechbal, F. Benhiba, A. Guenbour, B. Dikici, A. Zarrouk and A. Dafali, Anticorrosion effect of a green sustainable inhibitor on mild steel in hydrochloric acid, *J. Colloid Interface Sci.*, 2020, **580**, 740–752.

14 S. Kaya, C. Kaya, L. Guo, F. Kandemirlic, B. Tüzün, İ. Uğurlu, L. H. Madkour and M. Saraçoğlu, Quantum chemical and molecular dynamics simulation studies on inhibition performances of some thiazole and thiadiazole derivatives against corrosion of iron, *J. Mol. Liq.*, 2016, **219**, 497–504.

15 K. Efil and I. B. Obot, Quantum Chemical Investigation of the Relationship Between Molecular Structure and Corrosion Inhibition Efficiency of Benzotriazole and its Alkyl-Derivatives on Iron, *Prot. Met. Phys. Chem. Surf.*, 2017, **53**, 1139–1149.

16 M. Abdallah, K. A. Soliman, B. A. Al Jahdaly, J. H. Al-Fahemi, H. Hawsawi, H. M. Altass, M. Sobhi and S. S. Al-Juaid, Natural parsley oil as a green and safe inhibitor for corrosion of X80 carbon steel in 0.5M H2SO4 solution:

Chemical, electrochemical, DFT and MC simulation approach, *RSC Adv.*, 2022, **12**, 2959–2971.

17 F. M. Al-Nowaiser, M. Abdallah and E. H. El-Mossalamy, N,N-di (Polyoxyethylene)-4-dodecylaniline as an inhibitors of iron in hydrochloric acid solutions, *Chem. Technol. Fuels Oils*, 2012, **47**(6), 453–463.

18 M. Abdallah, K. A. Soliman, A. S. Al-Gorair, A. Al Bahir, J. H. Al-Fahemi, M. S. Motawea and S. S. Al-Juaid, Enhancing the inhibition and adsorption performance of SABIC iron corrosion in sulfuric acid by expired vitamins. Experimental and computational approach, *RSC Adv.*, 2021, **11**, 17092–17107.

19 M. Abdallah, I. Zaafarany, J. H. Al-Fahemi, Y. Abdallah and A. S. Fouda, Antibacterial cephalosporin as inhibitors for the corrosion of iron in hydrochloric acid solutions, *Int. J. Electrochem. Sci.*, 2012, **7**(8), 6622–6637.

20 N. I. Podobaev and Y. G. Avdeev, *Prot. Met.*, 2004, **40**, 7–13.

21 A. Fawzy, M. Abdallah, M. Alfakeer and H. M. Ali, Corrosion Inhibition of Sabic Iron in Different Media Using Synthesized Sodium N-dodecyl Arginine Surfactant, *Int. J. Electrochem. Sci.*, 2019, **14**, 2063–2084.

22 M. Abdallah, A. Al Bahir, H. M. Altass, A. Fawzy, N. El Guesmi, A. S. Al-Gorair, F. Benhiba, I. Warad and A. Zarrouk, Anticorrosion and adsorption performance of expired antibacterial drugs on Sabic iron corrosion in HCl solution: Chemical, electrochemical and Theoretical Approach, *J. Mol. Liq.*, 2021, **330**, 115702.

23 M. Abdallah, A. Fawzy and A. Al Bahir, The Effect of Expired Acyclovir and Omeprazole Drugs on the Inhibition of Sabic Iron Corrosion in HCl Solution, *Int. J. Electrochem. Sci.*, 2020, **15**, 4739–4753.

24 M. Abdallah, A. Fawzy and A. Al Bahir, Expired amoxicillin and cefuroxime drugs as efficient anticorrosive for Sabic iron in 1.0 M hydrochloric acid solution, *Chem. Eng. Commun.*, 2022, **209**(2), 158–170.

25 A. S. Al-Gorair, H. Hawsawi, A. Fawzy, M. Sobhi, A. M. Alharbi and R. S. Abdel Hameed, Evaluation of the Anticorrosion and Adsorption Properties of Polyethylene Glycol and Polyvinyl Alcohol for Corrosion of SABIC Iron in 1.0 M NaCl Solution, *Int. J. Electrochem. Sci.*, 2021, **16**, 211119, DOI: 10.20964/2021.11.03.

26 S. A. Umoren, Polymers as Corrosion Inhibitors for Metals in Different Media - A Review, *Open Corros. J.*, 2009, **2**, 175–188.

27 R. S. Abdel Hameed, A. El-Zomrawy, M. Abdallah, S. S. Abed El Rehim, H. I. AlShafey and N. I. Shaher, Polyoxyethylene stearate of molecular weight 6000 as corrosion inhibitor for mild steel in 2.0 M sulphuric acid, *International Journal of Corrosion and Scale Inhibition*, 2017, **6**, 196–208.

28 A. Ali, F. Sabirneeza, R. Geethanjali and S. Subhashini, Polymeric corrosion inhibitors for iron and its alloys: A Review, *Chem. Eng. Commun.*, 2015, **202**, 232–244.

29 F. M. Al-Nowaiser, M. Abdallah and E. H. El-Mossalamy, N,N-di (Polyoxyethylene)-4-dodecylaniline as an inhibitors of iron in hydrochloric acid solutions, *Chem. Technol. Fuels Oils*, 2012, **47**, 453–463.

30 D. E. Arthur, A. Jonathan, P. Ocheje Ameh and C. Anya, *Int. J. Ind. Chem.*, 2013, **4**, 2.

31 M. Abdallah, A. Fawzy and H. Hawsawi, Maltodextrin and Chitosan Polymers as Inhibitors for the Corrosion of Carbon Steel in in 1.0 M Hydrochloric Acid, *Int. J. Electrochem. Sci.*, 2020, **15**, 5650–5663.

32 M. Beniken, R. Salim, E. Ech-chihbi, M. Sfaira, B. Hammouti, M. Ebn Touhami, M. A. Mohsin and M. Taleb, Adsorption behavior and corrosion inhibition mechanism of a polyacrylamide on C–steel in 0.5 M H2SO4: Electrochemical assessments and molecular dynamic simulation, *J. Mol. Liq.*, 2022, **348**, 118022.

33 M. D. Shittu, J. O. Olawale, M. O. Adeoye, K. M. Oluwasegun, K. M. Adebayo and O. O. Ige, Investigation of Corrosion Resistance of Polystyrene as an Inhibitor in Hydrochloric and Tetra-oxo Sulphate VI Acids, *Int. J. Mater. Chem.*, 2014, **4**(1), 9–13.

34 M. M. Khowdiary, A. A. El-Henawy, A. M. Shawky and N. A. Negm, Synthesis and evaluation of novel corrosion inhibitors utilized from the recycling of polyethylene terephthalate polymer: Gravimetric, electrochemical, quantum chemical modeling, and molecular docking studies, *J. Mol. Liq.*, 2020, **320**(part B), 114504.

35 P. B. Mathur and T. Vasudevan, Reaction-rate studies for the corrosion of metals in acids: Iron in mineral acids, *Corrosion*, 1982, **38**, 17–25.

36 V. Barone and M. Cossi, Quantum calculation of Molecular Energies and Energy Gradient in Solution by a Conductor Solvent Model, *J. Phys. Chem. A*, 1988, **102**, 1995–2001.

37 M. J. Frisch, G. W. Trucks, H. B. Schlegel, G. E. Scuseria, M. A. Robb, J. R. Cheeseman, G. Scalmani, V. Barone, B. Mennucci, G. A. Petersson, H. Nakatsuji, M. Caricato, X. Li, H. P. Hratchian, A. F. Izmaylov, J. Bloino, G. Zheng, J. L. Sonnenberg, M. Hada, M. Ehara, K. Toyota, R. Fukuda, J. Hasegawa, M. Ishid, T. Nakajima, Y. Honda, O. Kitao, H. Nakai, T. Vreven, J. A. Montgomery, J. E. Peralta, F. Ogliaro, M. Bearpark, J. J. Heyd, E. Brothers, K. N. Kudin, V. N. Staroverov, T. Keith, R. Kobayashi, J. Normand, K. Raghavachari, A. Rendell, J. C. Burant, S. S. Iyengar, J. Tomasi, M. Cossi, N. Rega, J. M. Millam, M. Klene, J. E. Knox, J. B. Cross, V. Bakken, C. Adamo, J. Jaramillo, R. Gomperts, R. E. Stratmann, O. Yazyev, A. J. Austin, R. Cammi, C. Pomelli, J. W. Ochterski, R. L. Martin, K. Morokuma, V. G. Zakr-Zewski, G. A. Voth, P. Salvador, J. J. Dannenberg, S. Dapprich, A. D. Daniels, O. Farkas, J. B. Foresman, J. V. Ortiz, J. Cioslowski and D. J. Fox, Gaussian, Inc., Wallingford CT, 2010.

38 I.-C. Yeh and M. L. Berkowitz, Ewald summation for systems with slab geometry, *J. Chem. Phys.*, 1999, **111**, 3155–3162.

39 G. Quartarone, M. Battilana, L. Bonaldo and T. Tartato, Investigation of the inhibition effect of indole-3-carboxylic acid on the copper corrosion in 0.5 M H2SO4, *Corros. Sci.*, 2008, **50**, 3467–3474.

40 H. Gerengi and H. I. Sahin, *Schinopsis lorentzii* Extract As a Green Corrosion Inhibitor for Low Carbon Steel in 1 M HCl Solution, *Ind. Eng. Chem. Res.*, 2012, **51**, 780–788.

41 A. K. Singh and M. A. Quraishi, Inhibiting effects of 5-substituted isatin-based Mannich bases on the corrosion

of mild steel in hydrochloric acid solution, *J. Appl. Chem.*, 2010, **40**, 1293–1306.

42 M. Abdallah, B. H. Asghar, I. Zaafarany and M. Sobhi, Synthesis of some aromatic nitro compounds and its applications as inhibitors for corrosion of carbon steel in hydrochloric acid solution, *Prot. Met. Phys. Chem. Surf.*, 2013, **49**(4), 485–491.

43 M. Abdallah and A. I. Mead, Pitting corrosion of an iron electrode in HCO_3^-/Cl^- solutions and its inhibition by some non ionic surfactants, *Ann. Chim.*, 1993, **83**, 424–430.

44 M. Abdallah and S. M. Abd El-Haleem, Initiation and inhibition of pitting corrosion of Incoloy 800 and 316 Stainless Steel, *Bull. Electrochem.*, 1996, **12**(7–8), 449–458.

45 M. Abdallah, S. A. Al Karane and A. A. Abdel Fattah, Inhibition of the corrosion of nickel and its alloys by natural clove oil, *Chem. Eng. Commun.*, 2009, **196**, 1406–1416.

46 M. Sobhi, M. Abdallah and K. S. Khairou, Sildenafil citrate (Viagra) as a corrosion inhibitor for carbon steel in hydrochloric acid solutions, *Monatsh. Chem.*, 2012, **143**(10), 1379–1387.

47 M. Abdallah, H. M. Eltass, M. A. Hegazy and H. Ahmed, Adsorption and inhibition effect of novel cationic surfactant for pipelines carbon steel in acidic solutions, *Prot. Met. Phys. Chem. Surf.*, 2016, **52**(4), 721–730.

48 I. B. Obot, N. O. Obi-Egbedi and A. O. Eseola, Anticorrosion Potential of 2-Mesityl-1Himidazo[4,5-f][1,10]phenanthroline on Mild Steel in Sulfuric Acid Solution: Experimental and Theoretical Study, *Ind. Eng. Chem. Res.*, 2011, **50**, 2098–2110.

49 D. K. Yadav and M. A. Quraishi, Application of Some Condensed Uracils as Corrosion Inhibitors for Mild Steel: Gravimetric, Electrochemical, Surface Morphological, UV–Visible, and Theoretical Investigations, *Ind. Eng. Chem. Res.*, 2012, **51**, 14966–14979.

50 O. L. Riggs Jr and R. M. Hurd, Temperature coefficient of corrosion inhibition, *Corrosion*, 1967, **23**, 252–258.

51 K. J. Laider, *Chemical Kinetics*, Mc Graw Hill Publishing Company Ltd, 1965.

52 M. Abdallah and B. A. AL Jahdaly, Gentamicin, kanamycin and amikacin drugs as non -toxic inhibitors for corrosion of aluminum in 1.0M hydrochloric acid, *Int. J. Electrochem. Sci.*, 2015, **10**, 9808–9823.

53 S. Abd El Wanees, M. Abdallah, A. S. Al-Gorair, F. A. A. Tirkistani, S. Nooh and R. Assi, Kinetics and Thermodynamic Studies on the Anodic Passivation of Ni in H_2SO_4 Solutions by the Galvanostatic Polarization Method, *Int. J. Electrochem. Sci.*, 2021, **16**, 150969.

54 M. Abdallah, K. A. Soliman, R. Alfattani, A. S. Al-Gorair, A. Fawzy and M. A. A. Ibrahim, Insight of corrosion mitigation performance of SABIC iron in 0.5 M HCl Solution by tryptophan and histidine: Experimental and computational approaches, *Int. J. Hydrogen Energy*, 2022, **47**(2), 12782–12797.

55 A. Fawzy, I. A. Zaafarany, H. M. Ali and M. Abdallah, New Synthesized Amino Acids-based Surfactants as efficient inhibitors for corrosion of mild Steel in hydrochloric acid medium: Kinetics and thermodynamic approach, *Int. J. Electrochem. Sci.*, 2018, **13**, 4575–4600.

56 J. S. M. Anderson, J. Melin and P. W. Ayers, Conceptual Density-Functional Theory for General Chemical Reactions, Including Those That Are Neither Charge- nor Frontier-Orbital-Controlled. 1. Theory and Derivation of a General-Purpose Reactivity Indicator, *J. Chem. Theory Comput.*, 2007, **3**, 358–374.

57 M. Finsgar, A. Lesar, A. Kokalj and I. Milosev, A comparative electrochemical and quantum chemical calculation study of BTAH and BTAOH as copper corrosion inhibitors in near neutral chloride solution, *Electrochim. Acta*, 2008, **53**(28), 8287–8297.

58 F. Shojaie and N. Mirzai-Baghini, Molecular dynamics and density functional theory study on the corrosion inhibition of austenitic stainless steel in hydrochloric acid by two pyrimidine compounds, *Int. J. Ind. Chem.*, 2015, **6**, 297–310.

59 E. E. Ebenso, D. A. Isabirye and N. O. Eddy, Adsorption and Quantum Chemical Studies on the Inhibition Potentials of Some Thiosemicarbazides for the Corrosion of Mild Steel in Acidic Medium, *Int. J. Mol. Sci.*, 2010, **11**, 2473–2498.